Theory of the Galvanomagnetic Effects in Metals with Magnetic Breakdown: Semiclassical Approach*

L. M. FALICOV† AND PAUL R. SIEVERT‡
Department of Physics and Institute for the Study of Metals, University of Chicago, Chicago, Illinois
(Received 9 November 1964)

A new semiclassical method for calculating the galvanomagnetic tensor is presented; it allows for the inclusion of magnetic-breakdown effects, i.e., the possibility of coupled orbits is explicitly taken into account. Results of calculations for several cases based on various models of the Fermi-surface topology are given; they include most of the cases of physical interest regarding changes in the connectivity of the orbits. It is shown that in the very high-field region there exists an extra relaxation mechanism due to magnetic breakdown, which is a function of the energy gap.

I. INTRODUCTION

THE galvanomagnetic properties of metals have been widely used in the last decade to study the motion of conduction electrons in periodic structures.[1] In particular, measurements of the transverse magnetoresistance in single crystals as a function of magnetic field strength and as a function of angular orientation of both magnetic field and electric current have yielded a large amount of information on the topological properties of the Fermi surface. Two types of regimes have been distinguished: (a) the semiclassical regime, in which the electrons can be thought of as "classical" particles obeying Fermi-Dirac statistics and a general dispersion law $\epsilon(\mathbf{k})$; (b) the quantum-mechanical oscillatory regime, in which the quantization of the magnetic orbits (Landau levels) results in the well-known deHaas-Schubnikov and related effects.

Let us for the time being restrict ourselves to the semiclassical behavior. For large magnetic fields, two functional dependences of the magnetoresistance on magnetic field strength have been found experimentally[2]: (i) saturation, i.e., the resistance approaches a constant value as H is increased; (ii) quadratic behavior; i.e., resistance increases without bound proportionally to H^2. These two dependences have been interpreted in terms of the topology of energy surfaces and the results are summarized in Table I. For the sake of completeness, the behavior of the Hall voltage is also included in the table.

The theory that led to the interpretation of these experiments was based on the fundamental assumption that interband transitions, i.e., transitions between separate sheets of the Fermi surface, could be neglected from the start. However, this condition cannot always be met. Cohen and Falicov[3] and Blount[4] have proved that in metals in which an energy gap Δ is small enough to satisfy

$$K\Delta^2 mc/\epsilon_F eH\hbar = K\Delta^2/\epsilon_F \hbar\omega \lesssim 1, \qquad (1.1)$$

where ϵ_F is the Fermi energy, ω the cyclotron frequency, and K a numerical factor of order 1, the electrons have a finite probability of making a transition between the two energy bands separated by Δ. This phenomenon has been called *magnetic breakdown* and it has been found experimentally in various metals.[5–9] It has been recognized by the appearance at high fields of orbits which can only be obtained by repeated transitions between different pieces of the Fermi surface.

TABLE I. Magnetic-field dependence of the galvanomagnetic properties of metals in the high-field limit.

Type of orbits and state of compensation	Transverse magneto-resistance	Transverse Hall voltage
I. All closed orbits Uncompensated $n_e \neq n_h$	Saturates	$\propto \frac{H}{n_e - n_h}$
II. All closed orbits Compensated $n_e = n_h$	$\propto H^2$	$\propto H$
III. Open in direction perpendicular to H and making angle α with current	$\propto H^2 \cos^2\alpha$	$\propto H$

* Work supported in part by the National Science Foundation and the U. S. Office of Naval Research.
† Alfred P. Sloan Foundation Research Fellow.
‡ ARPA Research Assistant.

[1] For a complete summary of the theoretical and experimental situation see, for instance, R. G. Chambers in *The Fermi Surface*, edited by W. A. Harrison and M. B. Webb (John Wiley & Sons, Inc., New York, 1962), p. 100 and the many references quoted there.

[2] I. M. Litschitz, M. Ya. Azbel, and M. I. Kaganov, Zh. Eksperim. i Teor. Fiz. **30**, 220 (1955) [English transl.: Soviet Phys.—JETP **3**, 143 (1956)]; **31**, 63 (1956) [English transl.: Soviet Phys.—JETP **4**, 41 (1957)]. I. M. Lifshitz and V. G. Peschanskii, *ibid.* **35**, 1251 (1958) [English transl.: *ibid* **8**, 875 (1959)]; **38**, 188 (1960) [English transl.: Soviet Phys.—JETP **11**, 137 (1960)].

[3] M. H. Cohen and L. M. Falicov, Phys. Rev. Letters **7**, 231 (1961).

[4] E. I. Blount, Phys. Rev. **126**, 1636 (1962).

[5] Magnesium: M. G. Priestley, L. M. Falicov, and G. Weisz, Phys. Rev. **131**, 617 (1963); M. G. Priestley, Proc. Roy. Soc. (London) **A276**, 258 (1963); R. W. Stark, T. G. Eck, and W. L. Gordon, Phys. Rev. **133**, A443 (1964).

[6] Magnesium: R. W. Stark (private communication, and to be published).

[7] Zinc: R. W. Stark, Phys. Rev. **135**, A1698 (1964).

[8] Thallium: A. R. Mackintosh, L. E. Spanel, and R. C. Young, Phys. Rev. Letters **10**, 434 (1963); M. G. Priestley, Bull. Am. Phys. Soc. **9**, 239 (1964) (and to be published); P. Soven, Bull. Am. Phys. Soc. **9**, 239 (1964) (and to be published).

[9] Rhenium: A. S. Joseph and A. C. Thorsen, Phys. Rev. Letters **11**, 67 (1963).

The fact that the connectivity of the orbits can thus be drastically changed, together with the enormous differences that the connectivity produces in the transverse magnetoresistance at high fields, immediately points out that *new types of behavior* should be expected in the magnetic-field dependence of the resistivity tensor, whenever magnetic breakdown is present.[10]

In this paper we present a new method for computing the galvanomagnetic tensors in the semiclassical approximation for metals with magnetic breakdown, i.e., metals in which the orbits are coupled. The procedure here employed is a suitable matrix generalization of Chambers' path-integral method[11] for the solution of the Boltzmann equation. Section II is concerned with the details of the formalism. In Sec. III we present the results of several calculations based on various models of the Fermi-surface topology; they include most of the cases of physical interest as far as change in the connectivity is concerned. The general conclusions drawn from these calculations are discussed in Sec. IV. It should be noted that throughout this paper all quantum-oscillatory effects are neglected. These are in fact of major importance when the magnetic field is such that one or several pieces of the Fermi surface are in the deHaas-Schubnikov regime. Oscillatory contributions will be considered separately.[12]

II. METHOD OF CALCULATION

In order to compute the conductivity and resistivity tensors (σ_{ij} and ρ_{ij}) in the presence of large magnetic fields, the following assumptions will be explicitly made: (a) The electron distribution function f satisfies the Boltzmann equation, with the scattering term given by a relaxation time approximation:

$$(\partial f/\partial t)+(1/\hbar)\mathbf{F}\cdot(\partial f/\partial \mathbf{k})=-(f-f_0)/\tau. \quad (2.1)$$

Here $\mathbf{F}$ is the external force, f_0 the equilibrium Fermi-Dirac distribution function, and τ the relaxation time; independence of f on the space coordinates (uniformity) has been assumed.

(b) The force acting on the electron is the usual Lorentz force, i.e.,

$$\mathbf{F}=\hbar\dot{\mathbf{k}}=-|e|[\mathbf{E}+(1/c)\mathbf{v}\times\mathbf{H}]. \quad (2.2)$$

(c) The relaxation time is assumed to be constant on surfaces of constant energy. This assumption is good only in the high-magnetic-field region,[1] but since we are solely concerned with properties in that region, the approximation is introduced from the start.

(d) In the solution of (2.1), terms in the magnetic field $\mathbf{H}$ are included to all orders, but only terms linear in the electric field $\mathbf{E}$ are kept throughout. (Ohm's law regime.)

When assumptions (a)–(d) are taken into account, when use is made of Chambers' path integral method[11,13] for solving (2.1), and when the definition of the conductivity tensor σ_{ij} is kept in mind, i.e.,

$$J_i=\sum_j \sigma_{ij}E_j=-|e|\int v_i f d^3\mathbf{k}, \quad (2.3)$$

the well-known result[11]

$$\sigma_{ij}=-\frac{e^2}{4\pi^3}\int_{\text{all k}} v_i(\mathbf{k})\frac{df_0}{d\epsilon}d^3\mathbf{k}\int_{-\infty}^{t(\mathbf{k})} v_j(s)\exp\left[\frac{s-t}{\tau}\right]ds, \quad (2.4)$$

is obtained. In (2.4) it is understood that the time dependence of the velocity $v_j(s)$ is obtained from the set of equations

$$\hbar\dot{\mathbf{k}}=-(|e|/c)\mathbf{v}\times\mathbf{H}, \quad (2.5)$$

$$\mathbf{v}(\mathbf{k})=(1/\hbar)[\partial\epsilon(\mathbf{k})/\partial\mathbf{k}], \quad (2.6)$$

where the "equation of motion" (2.5) *does not* include the term due to the electric field.

In order to allow for the inclusion of magnetic-breakdown effects, two additional assumptions are made: (e) At a *finite number of points* in the orbit there may exist a finite probability of transition to (and from) another point in other orbits. These are the points where the energy gaps are small enough to permit an interband transition; they can also be considered the points at which the orbits become coupled to one another giving rise to a network of possible trajectories. It should be noted that two limits can always be defined, namely $H\to 0$ and $H\to\infty$; in both cases the orbits are decoupled but they are different in each limit. The orbits corresponding to $H\to\infty$ are those closer to the free-electron behavior, i.e., are those which at the transition points show no "Bragg reflection" due to the lattice potential. The orbits corresponding to $H\to 0$ are those obtained semiclassically by solving Eq. (2.5) and (2.6) for separate, isolated sheets of energy surface in which $\epsilon(\mathbf{k})$ has been determined by a Schrödinger equation in which the lattice potential is fully taken into account.

(f) The probability of transition between orbits is given by

$$P=\exp[-H_0/H], \quad (2.7)$$

where

$$H_0=K\Delta^2 mc/\epsilon_F e\hbar, \quad (2.8)$$

and all other symbols are defined in (1.1). Equation (2.7) was first derived by Blount[4] in the high-field limit as well as in the low-field limit; it has been proved[14,15] that it is valid for all magnetic fields.

[10] L. M. Falicov and P. R. Sievert, Phys. Rev. Letters **12**, 550 (1964).
[11] R. G. Chambers, Proc. Phys. Soc. (London) **A65**, 458 (1952); Proc. Roy. Soc. (London) **A238**, 344 (1956).
[12] L. M. Falicov, A. B. Pippard and P. R. Sievert (to be published).
[13] M. H. Cohen, M. J. Harrison, and W. A. Harrison, Phys. Rev. **117**, 937 (1960).
[14] J. R. Reitz, J. Phys. Chem. Solids **25**, 53 (1963).
[15] C. B. Duke and W. A. Harrison (private communication and to be published).

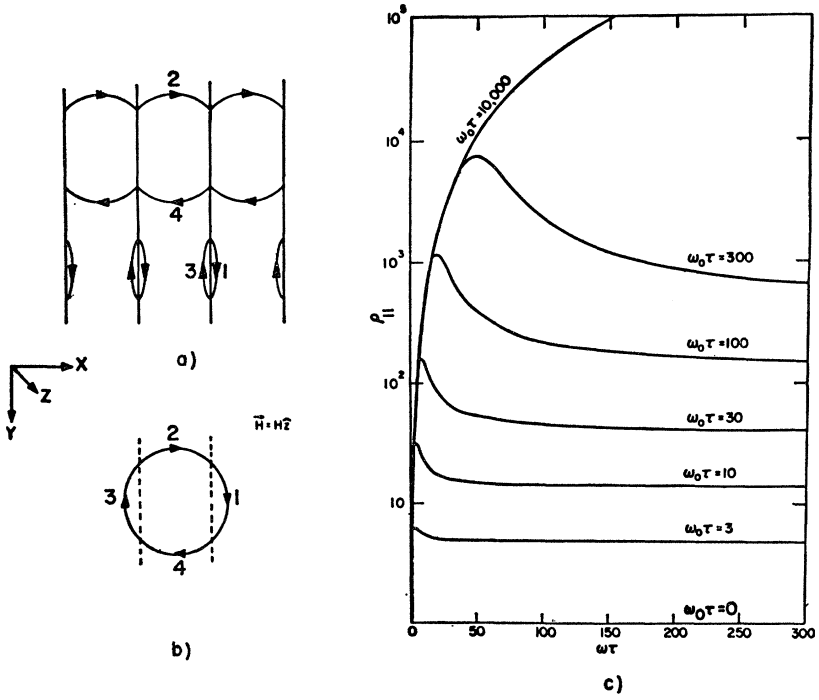

FIG. 1. Magnetoresistance for a transition from open orbits plus electron orbit to a closed (electron) orbit. (a) The orbits as $H \to 0$. (b) The orbit as $H \to \infty$. (c) The magnetoresistance parallel to the open orbits. All orbits refer to k space.

It is necessary now to include (e) and (f) in the calculation of the path integral

$$I_j(\mathbf{k}) = \exp[-t(\mathbf{k})/\tau] \int_{-\infty}^{t(\mathbf{k})} v_j(s) \exp(s/\tau) ds , \tag{2.9}$$

which is contained in (2.4). Once $I_j(\mathbf{k})$ is calculated the second integration over all $\mathbf{k}$ (over the Fermi surface only, in fact, due to the delta-function character of $df_0/d\epsilon$) can be carried on in a straightforward way.

In order to compute $I_j(\mathbf{k})$ and σ_{ij} we first choose $\mathbf{k}$ to be on a given energy surface (namely, the Fermi surface) and, by calling the z axis the direction of the magnetic field, restrict ourselves to a constant k_z. This choice of variables and application of (2.5) and (2.6) gives

$$d^3\mathbf{k} = (|e|H/\hbar^2 c) d\epsilon dt dk_z , \tag{2.10}$$

for each sheet of surface. In what follows only the dependence of $I_j(\epsilon, k_z, t)$ on t will be made explicit.

We now relabel the variable t in a more convenient way. Consider the complete network of orbits for given

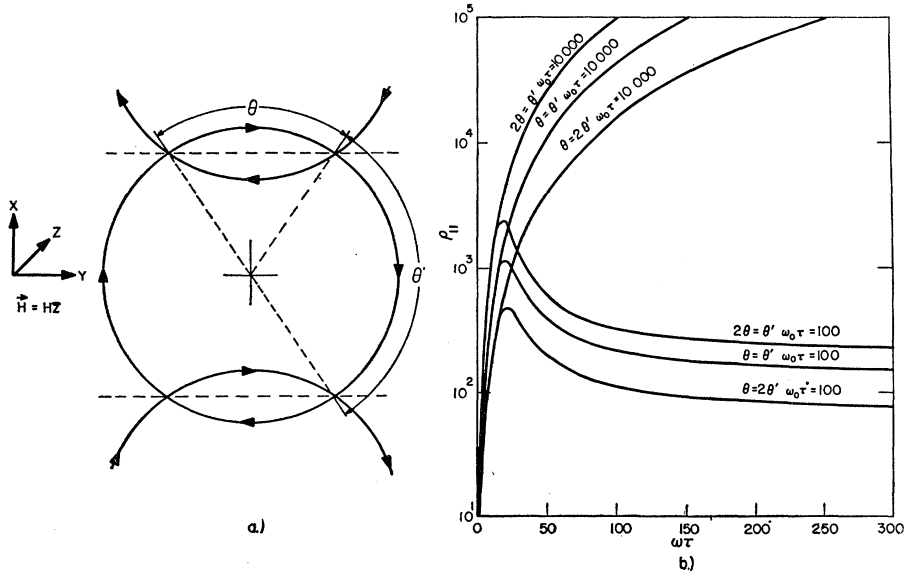

FIG. 2. Magnetoresistance for a transition from open orbits plus an electron orbit to a closed (electron) orbit. The $H \to 0$ relative size of the open orbits (θ') and the closed electron orbit (θ) are varied. (a) defines the parameters θ and θ'. (b) The magnetoresistance parallel to the open orbits for the values $\omega_0\tau = 10\,000$ and $\omega_0\tau = 100$ of the breakdown parameter and for $\theta = 2\theta'$, $\theta = \theta'$, $2\theta = \theta'$.

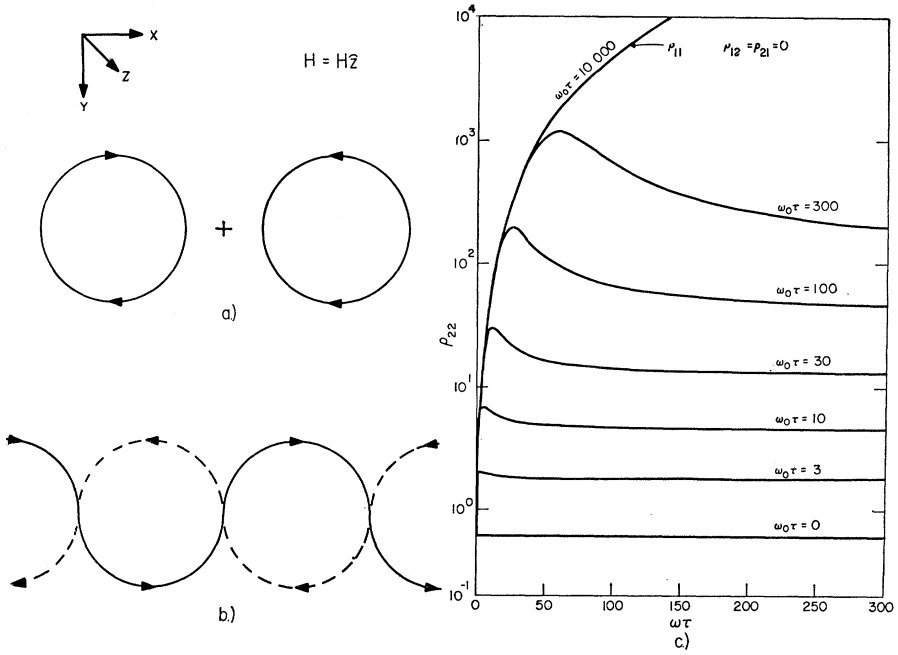

FIG. 3. Magnetoresistance for a transition from compensated closed orbits to two intersecting open orbits. (a) The orbits as $H \to 0$. (b) Orbits as $H \to \infty$. (c) The magnetoresistance perpendicular to the open orbits.

ϵ, k_z and divide it into a *finite* number n of isochronous pieces, i.e., pieces that are travelled by the electrons all *in the same length of time* t_0. All points at which breakdown is possible should coincide with end-points of the isochronous pieces.[16] The pieces are now labeled by an index l running from 1 to n. The variable t is thus labeled by two numbers t' and l, where l indicates the particular piece of orbit and t' is measured from one of the end points and reaches the value t_0 at the other. With this new nomenclature (2.4) reduces to

$$\sigma_{ij}=-\frac{e^2m\omega}{4\pi^3\hbar^2}\sum_{l=1}^{n}\int\frac{df_0}{d\epsilon}d\epsilon\int dk_z\int_0^{t_0}v_i(t',l)I_j(t',l)dt'. \tag{2.11}$$

If now we apply the formalism to the trivial case of a single sheet of Fermi surface (with no breakdown) in which the artificially divided pieces are numbered consecutively, (2.9) can be re-expressed as

$$I_j(t',l)=\exp(-t'/\tau)\left\{\int_0^{t'}v_j(s',l)\exp(s'/\tau)ds'+K_j(l)\right\}, \tag{2.12}$$

$$K_j(l)=\sum_{p=1}^{\infty}\int_0^{t_0}v_j(s',l-p)\exp[(s'-pt_0)/\tau]ds', \tag{2.13}$$

in which $(l-p)$ is determined modulo n. It is now useful to define $\mathbf{K}_j$ a column vector of n components $K_j(l)$, $\mathbf{V}_j$ another column vector of n components

$$V_j(r)=\int_0^{t_0}v_j(s',r)\exp(s'/\tau)ds',\quad r=1,2,\cdots n, \tag{2.14}$$

and $\mathbf{M}$, and $n\times n$ square matrix of elements

$$M_{lr}=\delta_{l,r-1},\qquad l,\ r \text{ modulo } n. \tag{2.15}$$

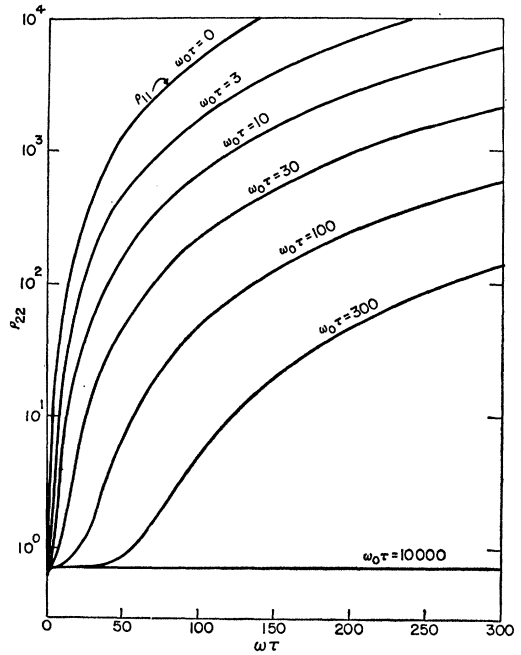

FIG. 4. Magnetoresistance for a transition from open orbits plus closed orbits to closed compensated orbits. The orbits at both limits, except for the compensating holes, are identical to Figs. 1(a) and (b), respectively. The graph shows the magnetoresistance perpendicular to the open orbits.

[16] We have assumed that the times taken by the electrons to travel between consecutive breakdown points are in rational ratios to one another; this assumption is of course of no consequence from the physical viewpoint, since a general irrational case can be approximated as much as desired by rational ratios.

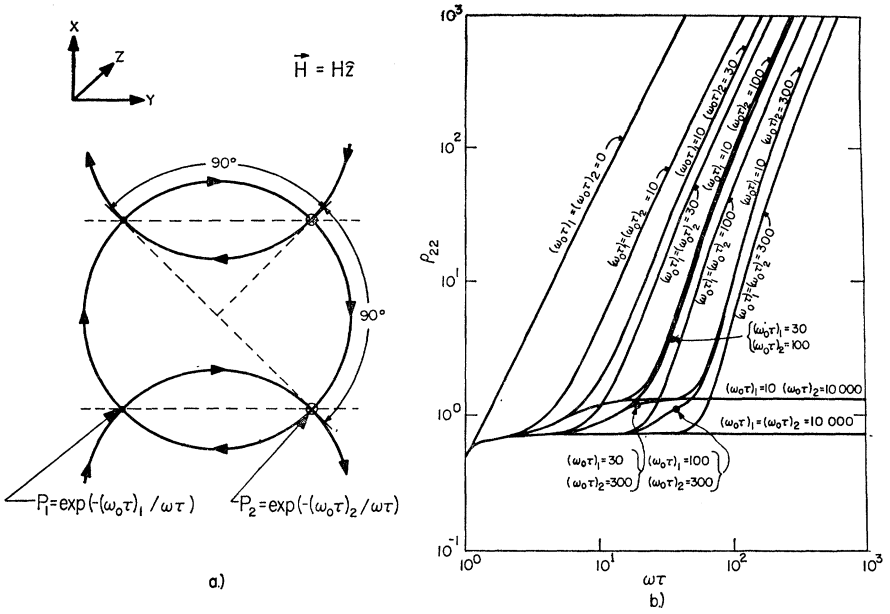

FIG. 5. Magnetoresistance for a transition from open oribts to closed compensated orbits with two simultaneous different breakdown probabilities. (a) defines the points of transition and the breakdown probabilities; (b) the magnetoresistance perpendicular to the open orbits for various values of the breakdown parameters.

In this fashion (2.13) is rewritten

$$\mathbf{K}_j = \sum_{p=1}^{\infty} \mathbf{M}^p \cdot \mathbf{V}_j \exp(-pt_0/\tau)$$

$$= \mathbf{M} \exp(-t_0/\tau) \cdot [\mathbf{1} - \mathbf{M} \exp(t_0/\tau)]^{-1} \cdot \mathbf{V}_j, \quad (2.16)$$

where $\mathbf{1}$ is the $n \times n$ identity matrix.

The final solution is given by insertion of (2.16) and (2.12) into (2.11). This method in the trivial case discussed above is, of course, unnecessarily complicated. However, it is capable of immediate generalization to cases with magnetic breakdown by only changing the definition (2.15) of the matrix $\mathbf{M}$. In this generalization the element M_{lr} is given by the probability that the electron which goes into piece l will come from piece r. That is, in general the matrix elements M_{lr} will be equal to 1, 0, P or $Q=(1-P)$, depending on the network considered as well as on the pieces l and r.

In order to be specific we show in detail the example first discussed in connection with magnetic breakdown

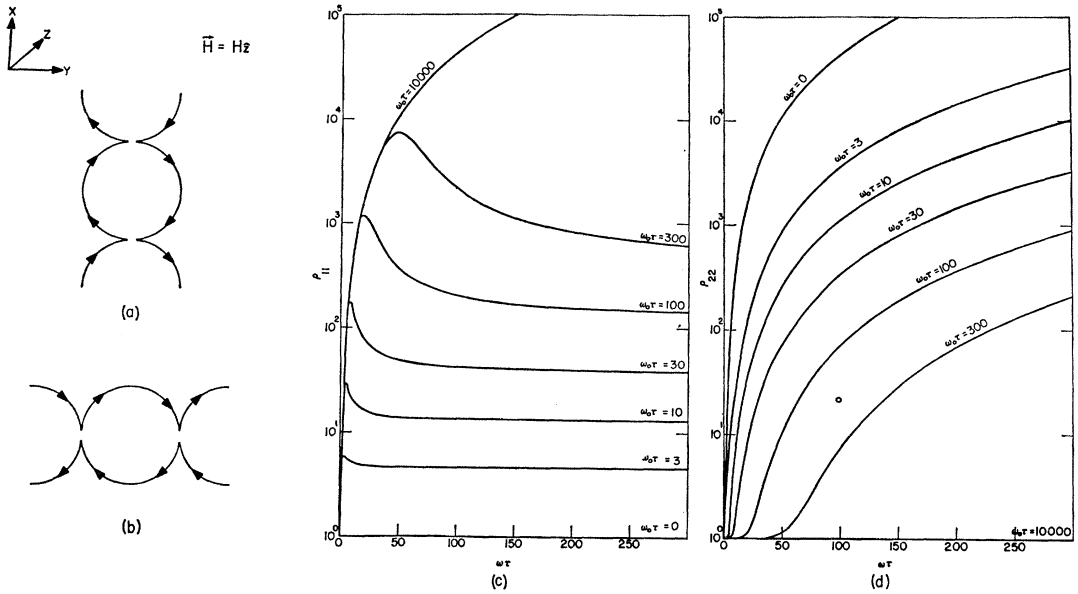

FIG. 6. Magnetoresistance for a transition from open orbits in a given direction to open orbits perpendicular to them. (a) The orbits as $H \to 0$; (b) the orbits as $H \to \infty$; (c) the magnetoresistance parallel to the original open orbits, i.e., those as $H \to 0$; (d) the magnetoresistance perpendicular to the original open orbits.

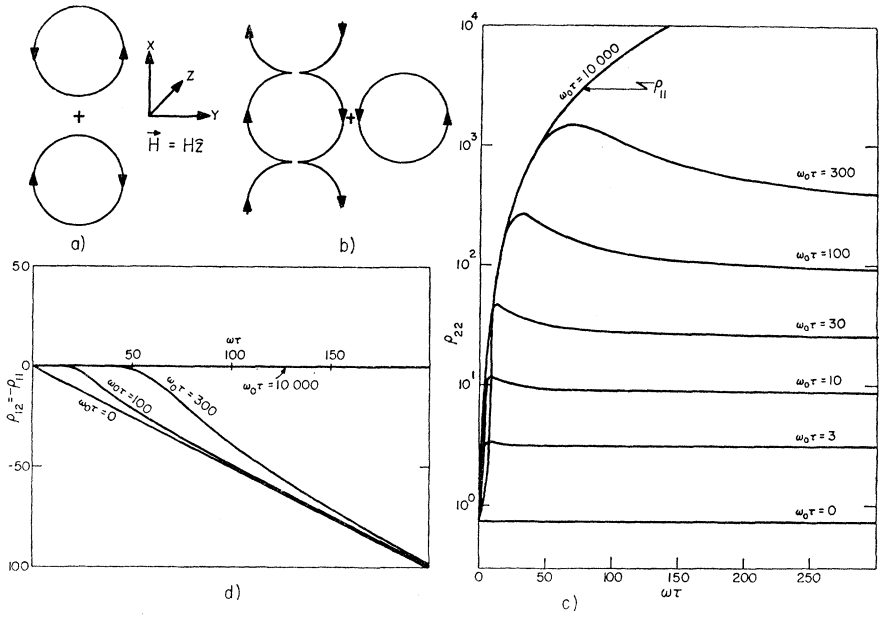

FIG. 7. Magnetoresistance and Hall resistance for transitions from closed compensated orbits to open and closed (hole) orbits. (a) The orbits as $H \to 0$; (b) the orbits as $H \to \infty$; (c) the magnetoresistance perpendicular to the open orbits; (d) the Hall resistance.

by Cohen and Falicov,[3] and Pippard.[17] It is shown in Fig. 1 and corresponds to the transition from two open orbits and a "lens"-shaped electron orbit at $H \to 0$ [Fig. 1(a)], to a circular electron orbit as $H \to \infty$ [Fig. 1(b)]. For simplicity in the matrix calculation we have assumed a constant Fermi velocity in the orbit and pieces of equal length in the lens and the open orbits. If the pieces are numbered counterclockwise as in Fig. 1(b), the sequences which give the uncoupled orbits are

$$\begin{matrix} 1\text{-}3\text{-}1\text{-}3\text{-}1\text{-}3\text{-}\cdots \\ 2\text{-}2\text{-}2\text{-}2\text{-}2\text{-}2\text{-}\cdots \quad H \to 0, \\ 4\text{-}4\text{-}4\text{-}4\text{-}4\text{-}4\text{-}\cdots \end{matrix} \tag{2.17}$$

and

$$1\text{-}4\text{-}3\text{-}2\text{-}1\text{-}4\text{-}3\text{-}2\text{-}1\text{-}\cdots H \to \infty. \tag{2.18}$$

These sequences correspond to a general matrix

$$\mathbf{M} = \begin{pmatrix} 0 & P & Q & 0 \\ 0 & Q & P & 0 \\ Q & 0 & 0 & P \\ P & 0 & 0 & Q \end{pmatrix}, \tag{2.19}$$

where P is given by (2.7) and $Q = 1 - P$. Insertion of (2.19) and (2.7) into (2.16), (2.12), and (2.11) gives σ_{ij} and, by inverting the tensor, ρ_{ij}. The final result ρ_{11} is shown in Fig. 1(c).

Before concluding these general remarks on the method it is worth noticing that the summation in (2.16) always converges due to the general form of the matrix $\mathbf{M}$ and the converging factor given by the exponential. The summation of the geometric series results in a matrix inversion, as is apparent in (2.16) and consequently the amount of computation required is roughly proportional to n^2. For most cases but the trivial ones, calculations by hand become prohibitive and it is necessary to invert the matrix and evaluate the formulas numerically; for the examples described in the next section the calculations were carried out in the IBM 7094 complex of the University of Chicago Computation Center.

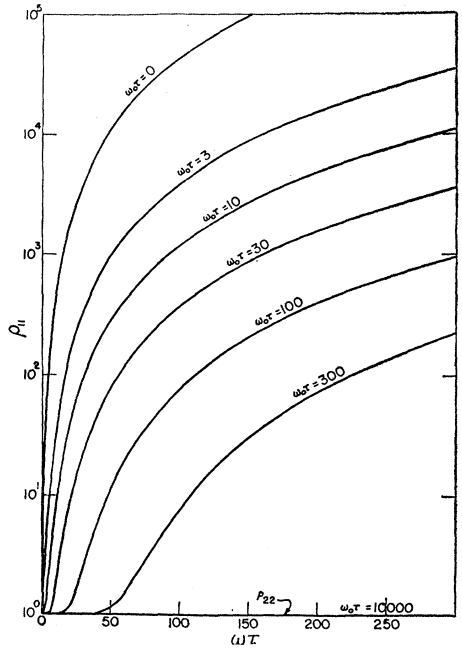

FIG. 8. Magnetoresistance for a transition from a closed (electron) orbit to open orbits. The orbits at both limits, if the compensating hole orbit is omitted, are identical to Figs. 7(a) and (b), respectively. The graph shows the magnetoresistance parallel to the open orbits.

[17] A. B. Pippard, Proc. Roy. Soc. (London) **A270**, 1 (1962); Phil. Trans. Roy. Soc. London **A256**, 317 (1964).

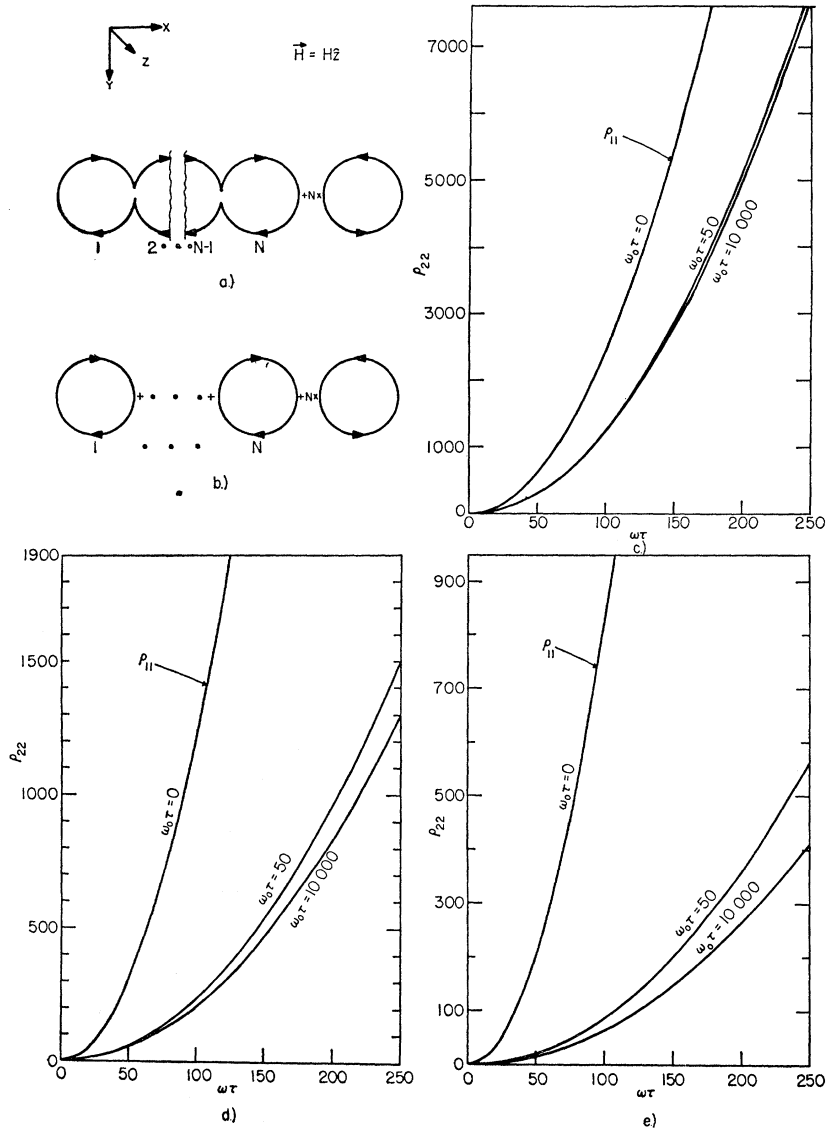

FIG. 9. Magnetoresistance for a transition from a closed extended (electron) orbit constructed of $2N$ semicircular orbits and N closed (hole) orbits, to N closed (electron) orbits and N compensating closed (hole) orbits. (a) The orbits as $H \to 0$; (b) the orbits as $H \to \infty$; (c) the magnetoresistance perpendicular to the major axis of the extended orbit for $N=2$; (d) for $N=4$; (e) for $N=6$.

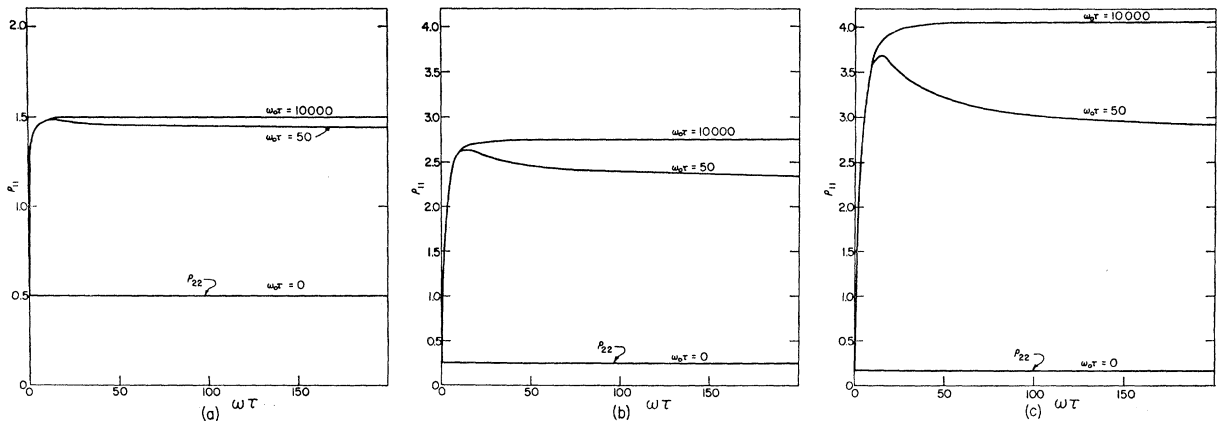

FIG. 10. Magnetoresistance for transitions from a closed extended (electron) orbit constructed of $2N$ semicircular orbits to N closed (electron) orbits. (a) The magnetoresistance parallel to the major axis of the extended orbit for $N=2$. (b) $N=4$; (c) $N=6$.

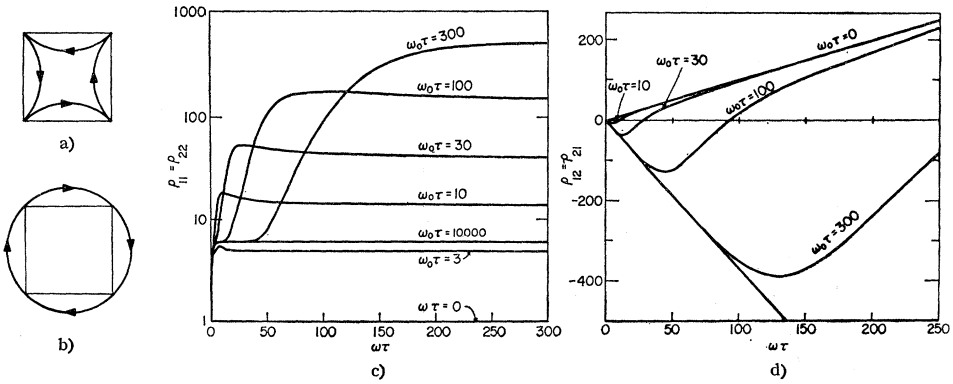

FIG. 11. Magnetoresistance and Hall resistance for a transition from a closed (hole) orbit to a closed (electron) orbit. (a) The orbit as $H \to 0$; (b) the orbit as $H \to \infty$; (c) the magnetoresistance; (d) the Hall resistance.

III. MODEL CALCULATIONS

Figures 1 to 16 show the results of various calculations corresponding to several models. They include most of the cases of physical interest as far as connectivity and symmetry are concerned. The figures together with the figure captions are in general self-explanatory.

Figures 1 to 10 include cases of low (twofold or mirror) symmetry, Figs. 11 to 13 correspond to fourfold symmetry, and Figs. 14 to 16 are sixfold symmetric.

For the case of uncoupled orbits, i.e., no magnetic breakdown or complete magnetic breakdown, four different cases of interest can be found:

I. compensated closed orbits, i.e., equal number of electrons and holes;
II. uncompensated closed orbits of the electron type;
III. uncompensated closed orbits of the hole type;
IV. open orbits.

When magnetic breakdown couples the orbits, sixteen different possibilities appear; of these, twelve are equivalent in pairs, giving a net number of ten essentially different cases. All these are included in the studied cases and are divided in the following way:

I → I	Fig. 9
I → II (or I → III)	Figs. 12, 14, 15, and 16
I → IV	Figs. 3 and 7
II → I (or III → I)	Fig. 13
II → II (or III → III)	Fig. 10
II → III (or III → II)	Fig. 11
II → IV (or III → IV)	Fig. 8
IV → I	Figs. 4 and 5
IV → II (or IV → III)	Figs. 1 and 2
IV → IV	Fig. 6.

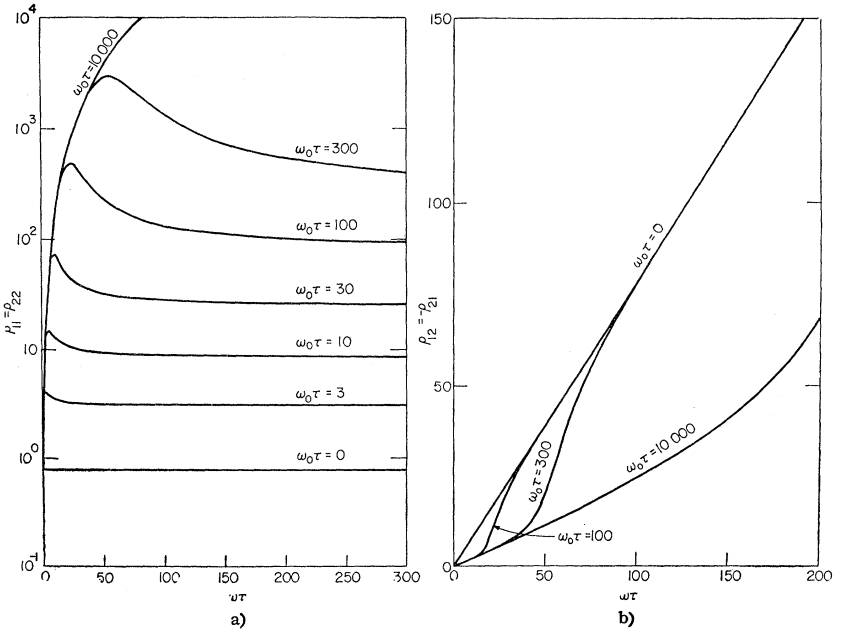

FIG. 12. Magnetoresistance and Hall resistance for a transition from compensated closed orbits to closed electron orbits. The orbits at both limits, except for the compensating (electron) orbit are identical to Figs. 12 (a) and (b), respectively; (a) the magnetoresistance; (b) the Hall resistance.

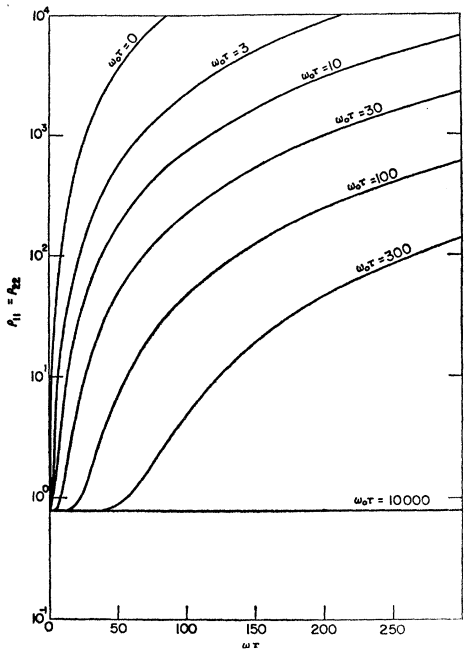

FIG. 13. Magnetoresistance for a transition from closed (electron) orbits to closed compensated orbits. The orbits at both limits, except for the compensating (electron) orbit, are identical to Figs. 11 (b) and (a), respectively. The graph shows the magnetoresistance.

We have indicated by an arrow the transition between the various types from that as $H \rightarrow 0$ (before the arrow) to that as $H \rightarrow \infty$ (after the arrow).

All models computed and reported here correspond to orbits formed by arcs of circle with Fermi velocities of constant magnitude. In addition no k_z dependence has been included, i.e., all relevant contributions to σ_{ij} are supposed to arise from a small "cylindrical" slab of the Fermi surface. Each curve is labeled by a parameter $\omega_0\tau$ and is plotted as a function of $\omega\tau$, where

$$\omega\tau=(|e|H\tau/mc), \qquad \omega_0\tau=(|e|H_0\tau/mc); \quad (3.1)$$

both parameters are dimensionless.

Figures 14 to 16 need some further explanation. The three figures are sixfold symmetric. Figures 14 and 15 correspond to a 6×6 matrix $\mathbf{M}$, while Fig. 16 is obtained from a 12×12 matrix. Figure 14 arises from the unphysical assumption that at each corner α only two possible trajectories exist; this results in a matrix

$$\mathbf{M}=\begin{pmatrix} 0 & P & 0 & 0 & 0 & Q \\ Q & 0 & P & 0 & 0 & 0 \\ 0 & Q & 0 & P & 0 & 0 \\ 0 & 0 & Q & 0 & P & 0 \\ 0 & 0 & 0 & Q & 0 & P \\ P & 0 & 0 & 0 & Q & 0 \end{pmatrix}, \quad (3.2)$$

which in turn gives rise to the magnetoresistance and Hall resistance there shown.

Figure 15 on the other hand may correspond very closely to the case of zinc for H parallel to the hexad axis, if oscillations are neglected. In this case each corner α of the hexagon [Fig. 14(a)] is supposed to have an infinitesimally small triangular needle from which a "three-way switch" is obtained. The cor-

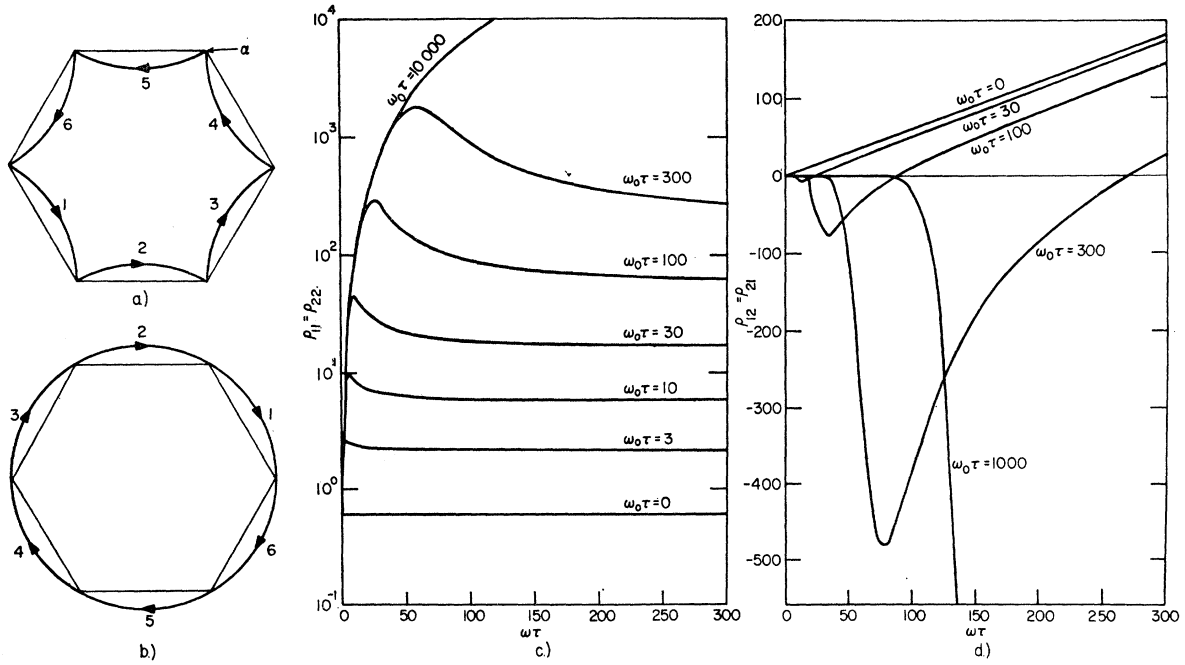

FIG. 14. Magnetoresistance and Hall resistance for a transition from closed compensated orbits to closed (electron) orbits. (a) The compensated hole orbit as $H \rightarrow 0$; (b) one electron orbit as $H \rightarrow \infty$; (c) the magnetoresistance; (d) the Hall resistance. The matrix M for this case is given by (3.2).

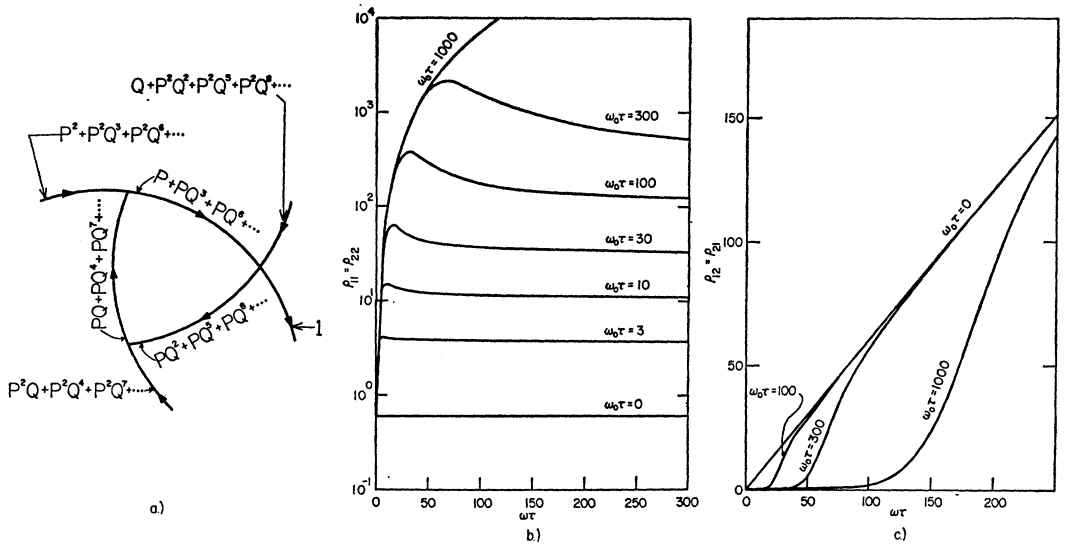

FIG. 15. Magnetoresistance and Hall resistance for a transition from closed compensated orbits to closed (electron) orbits. The orbits at both limits, except for the compensating (electron) orbit, are identical to Figs. 14(a) and (b), respectively. This model includes infinitesimal "needles" at the corners of the hexagon of Fig. 14(a). (a) The details of calculating the breakdown probabilities for the "needle"; (b) the magnetoresistance; (c) the Hall resistance. The matrix **M** is given by (3.3) and (3.4).

responding matrix is

$$\mathbf{M}=\begin{pmatrix} 0 & B & 0 & C & 0 & A \\ A & 0 & B & 0 & C & 0 \\ 0 & A & 0 & B & 0 & C \\ C & 0 & A & 0 & B & 0 \\ 0 & C & 0 & A & 0 & B \\ B & 0 & C & 0 & A & 0 \end{pmatrix}. \tag{3.3}$$

It is evident from Fig. 14(a) that

$$A=Q+P^2Q^2+P^2Q^5+\cdots=Q+P^2Q^2/(1-Q^3),$$
$$B=P^2+P^2Q^3+P^2Q^6+\cdots=P^2/(1-Q^3),$$
$$C=P^2Q+P^2Q^4+P^2Q^7+\cdots=P^2Q/(1-Q^3), \tag{3.4}$$

so that

$$A+B+C=1. \tag{3.5}$$

In Fig. 16 the size of the triangular pieces is finite and the length of each side equal to the length of the central

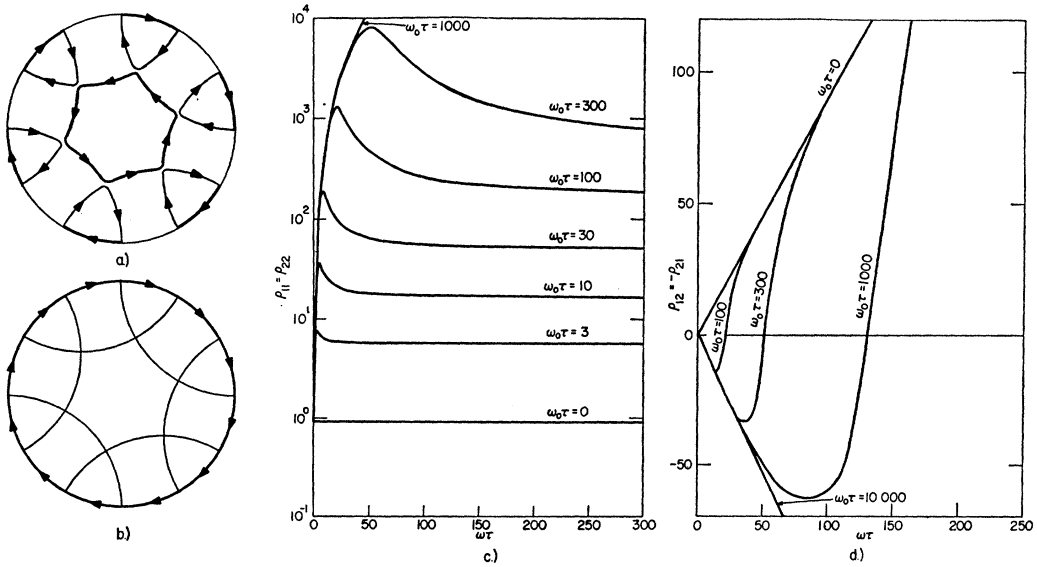

FIG. 16. Magnetoresistance and Hall resistance for a transition from closed compensated orbits to closed (electron) orbits. This model includes finite "cigars." (a) The orbits as $H \rightarrow 0$ neglecting a compensating (electron) orbit; (b) the orbit as $H \rightarrow \infty$ again neglecting the compensating (electron) orbit; (c) the magnetoresistance; (d) the Hall resistance.

"hexagon." This case is similar to the magnetoresistance of magnesium for H parallel to the c axis. It is worth pointing out that Figs. 15(b) and 16(c), i.e., the transverse magnetoresistances, have a very close resemblance, whereas Figs. 15(c) and 16(d), the transverse Hall resistances, show considerable differences. These effects have been found experimentally in Mg[5] and Zn.[7] It should be added that inclusion of the oscillations in these curves[12] brings the theory into very good agreement with experiment.

IV. CONCLUSIONS

From the results shown in the previous section, several general conclusions can be drawn.

(a) Those cases which start with quadratic behavior and break down to saturated magnetoresistance, saturate at a value of ρ much higher in general than the zero field value. Detailed calculations show that

$$\rho_{\text{sat}} \propto (\tau^{-1}+C\omega_0), \tag{4.1}$$

where τ is the relaxation time, ω_0 is given by (3.1) and C is a constant of order unity. This result can be interpreted in terms of an effective non-Markovian relaxation time τ_{eff} given by

$$1/\tau_{\text{eff}}=(1/\tau)+C\omega_0 \tag{4.2}$$

valid for high fields.[18]

The constant C takes for instance the value $4/\pi$ in Fig. 1, 1 in Fig. 11, $\sqrt{3}/2$ in Fig. 14 and $\sqrt{3}$ in Figs. 15 and 16.

As an interesting example, the case corresponding to Fig. 2 with $\theta \to 0, \theta' \to 180°$, which is a 2×2 case, can be computed analytically in closed form.[19] In particular, in the limit $\tau \to \infty$ the transverse resistivity tensor reduces to

$$\varrho=\begin{pmatrix} \dfrac{m}{e^2 n\tau_1} & \dfrac{H}{nec} \\ -\dfrac{H}{nec} & 0 \end{pmatrix}, \tag{4.3}$$

where m is the electron mass, n the number of electrons per unit volume, and

$$1/\tau_1=(8/\pi)\omega(1-P)/P=(8/\pi)\omega[\exp(\omega_0/\omega)-1]. \tag{4.4}$$

This additional relaxation time can be interpreted in the following simple terms. As $H \to \infty$ the probability of the electron being scattered off the free-electron orbit at each transition point is given by

$$Q=1-P=1-\exp(-\omega_0/\omega)\cong\omega_0/\omega. \tag{4.5}$$

However, since the frequency ω increases linearly with H, the probability of scattering per unit time, i.e., the inverse of the effective relaxation time, is proportional to $\omega Q\cong\omega_0$, that is, it approaches a constant value.

(b) The resistivity tensor as a function of $\omega\tau$ does not scale with the parameter $\omega_0\tau$. This gives rise to a dependence of the "shape" of the curves on the purity of the sample. For example, (4.1) shows that ρ_{sat} is only slightly dependent on τ for $\omega_0\tau \gg 1$; on the other hand the position of the maximum ω_m of the curves satisfied a relation of the form

$$\omega_0\cong A\omega_m+B\omega_m\tau, \tag{4.6}$$

where A and B are positive numerical constants. It is seen that as τ increases the maximum moves to smaller values of ω. This has also been found experimentally in Zn[7] and Mg.[5]

(c) The position of the maximum $\omega_m=(eH_m/mc)$ is not a good indication of the value of the magnetic-breakdown parameter H_0, since H_m, as shown in (4.6) is only a fraction of H_0.

In conclusion we would like to point out that the present formulation can be extended (i) to include oscillations due to small pieces of the Fermi surface by considering phase-coherence effects[12,17]; (ii) to include coupling of orbits at an infinite number of points by changing the matrix formulation into an integral equation formulation with a continuous probability of transition between any two points of the generalized orbit.

ACKNOWLEDGMENTS

The authors would like to acknowledge several stimulating discussions and exchange of information with Professor M. H. Cohen, Dr. E. Fawcett, Professor A. B. Pippard, F.R.S., Professor M. G. Priestley, Dr. P. Soven, and Professor R. W. Stark.

We are grateful to the National Science Foundation and the Office of Naval Research for direct financial support of this work. In addition, the research benefited from partial support of related solid-state theory by NASA and general support of the Institute for the Study of Metals by ARPA and the NSF.

[18] The existence of the extra relaxation mechanism has been previously pointed out by W. A. Harrison, Phys. Rev. **126**, 497 (1962).

[19] In the limit $\theta \to 0$ $\theta' \to 180°$ the matrix $\mathbf{M}$ reduces to

$$\mathbf{M}=\begin{pmatrix} \dfrac{2Q}{1+Q} & \dfrac{P}{1+Q} \\ \dfrac{P}{1+Q} & \dfrac{2Q}{1+Q} \end{pmatrix},$$

which is obtained in a fashion similar to the case of Fig. 15(a) and formulae (3.4) and (3.5). We are grateful to Professor A. B. Pippard for pointing this out.